Arc restores juvenile plasticity in adult mouse visual cortex

Massachusetts Institute of Technology

Arc restores juvenile plasticity in adult mouse visual cortex

Kyle R. Jenks[a,1], Taekeun Kim[b,1], Elissa D. Pastuzyn[a,1], Hiroyuki Okuno[c,d], Andrew V. Taibi[a], Haruhiko Bito[d], Mark F. Bear[b,2], and Jason D. Shepherd[a,2]

[a]Department of Neurobiology and Anatomy, University of Utah, Salt Lake City, UT 84112; [b]The Picower Institute for Learning and Memory, Massachusetts Institute of Technology, Cambridge, MA 02139; [c]Medical Innovation Center, Kyoto University Graduate School of Medicine, Sakyo-ku, Kyoto 606-8507, Japan; and [d]Department of Neurochemistry, Graduate School of Medicine, The University of Tokyo, Hongo 7-3-1, Bunkyo-ku, Tokyo 113-0033, Japan

The molecular basis for the decline in experience-dependent neural plasticity over age remains poorly understood. In visual cortex, the robust plasticity induced in juvenile mice by brief monocular deprivation during the critical period is abrogated by genetic deletion of Arc, an activity-dependent regulator of excitatory synaptic modification. Here, we report that augmenting Arc expression in adult mice prolongs juvenile-like plasticity in visual cortex, as assessed by recordings of ocular dominance (OD) plasticity in vivo. A distinguishing characteristic of juvenile OD plasticity is the weakening of deprived-eye responses, believed to be accounted for by the mechanisms of homosynaptic long-term depression (LTD). Accordingly, we also found increased LTD in visual cortex of adult mice with augmented Arc expression and impaired LTD in visual cortex of juvenile mice that lack Arc or have been treated in vivo with a protein synthesis inhibitor. Further, we found that although activity-dependent expression of *Arc* mRNA does not change with age, expression of Arc protein is maximal during the critical period and declines in adulthood. Finally, we show that acute augmentation of Arc expression in wild-type adult mouse visual cortex is sufficient to restore juvenile-like plasticity. Together, our findings suggest a unifying molecular explanation for the age- and activity-dependent modulation of synaptic sensitivity to deprivation.

Arc | synaptic plasticity | visual cortex | ocular dominance | critical period

A defining feature of early postnatal brain development is the activity-dependent winnowing of synaptic connections. This process is readily demonstrated by the response of visual cortical circuits to temporary monocular deprivation (MD) during early life. When MD is initiated during an early critical period, the synapses serving the deprived eye in visual cortex lose strength and are eliminated. Deprived-eye depression diminishes with age such that by the onset of adolescence, circuits are less vulnerable to the effects of deprivation. Understanding the molecular mechanisms that underlie the effect of age on this type of ocular dominance (OD) plasticity is considered one of the great challenges in neuroscience (1).

It is now well established that OD plasticity after MD occurs through synaptic plasticity of excitatory transmission, using mechanisms that include homosynaptic long-term depression (LTD), metaplasticity, and homeostatic scaling of AMPA-type glutamate receptors (2, 3). Clues to the molecular basis for the decline in juvenile plasticity have come from several diverse experimental treatments that can restore or prolong sensitivity to MD in adult animals. These include genetic manipulations that slow the maturation of cortical inhibition (4, 5), enrichment of animal housing conditions (6), increased exposure to visual stimulation (7), and enhanced modulatory neurotransmission (8). It has been suggested that a common thread connecting these varied treatments might be an increase in the ratio of excitation to inhibition (9, 10). However, it is completely unknown how, at the molecular level, general increases in cortical activity can facilitate deprivation-induced synaptic plasticity in adult visual cortex. Since the immediate early gene Arc is exquisitely sensitive to changes in cortical activity, and is essential for both OD plasticity and modification of excitatory

synaptic transmission (11–13), we set out to determine whether availability of Arc limits or changes the qualities of plasticity in adults and whether up-regulating Arc levels in adult animals can restore juvenile synaptic plasticity.

Results

Augmentation of Arc Expression in Adult Mouse Visual Cortex Extends the Critical Period of Juvenile OD Plasticity. In young mice [≤ postnatal day (P) 40], the main consequence of short (3–4 d) MD is the robust loss of cortical responsiveness to stimulation of the deprived eye. A compensatory potentiation of responses to the nondeprived eye may also occur, and is typically observed with longer periods of MD (5–7 d) (14). Importantly, although open-eye potentiation after long-duration MD is common in adult rodents, deprived-eye depression typically is only observed during the juvenile critical period in animals housed under standard laboratory conditions (15, 16). We predicted that augmenting Arc levels would prolong juvenile plasticity, as defined by closed-eye depression, past the conventional critical period in mouse visual cortex. To test this hypothesis, we used a transgenic (Tg) mouse line that expresses an additional allele of *Arc* tagged with mCherry that is driven by the activity-dependent *Arc* promoter in a similar manner to the previously characterized Arc-GFP Tg mouse line (17, 18) (Fig. S1).

We compared the qualities of OD plasticity after short (3–4 d) MD in Arc-Tg mice and wild-type (WT) littermate controls at P30 (juvenile) and P180 (adult) using chronic recordings of

Significance

Neuronal plasticity peaks early in life during critical periods and normally declines with age, but the molecular changes that underlie this decline are not fully understood. Using the mouse visual cortex as a model, we found that activity-dependent expression of the neuronal protein Arc peaks early in life, and that loss of activity-dependent Arc expression parallels loss of synaptic plasticity in the visual cortex. Genetic overexpression of Arc prolongs the critical period of visual cortex plasticity, and acute viral expression of Arc in adult mice can restore juvenile-like plasticity. These findings provide a mechanism for the loss of excitatory plasticity with age, and suggest that Arc may be an exciting therapeutic target for modulation of the malleability of neuronal circuits.

visually evoked potentials (VEPs) from binocular visual cortex contralateral (contra) to the deprived eye (Fig. 1*A*) as previously described (11). There was no significant difference between P30 WT and Arc-Tg VEPs before MD, and following MD, both WT and Arc-Tg P30 mice exhibited a significant decrease in contra (closed-eye) VEP amplitudes (WT: $n = 7$, baseline = 251 ± 28 µV, post-MD = 166 ± 12 µV, $P = 0.03$; Arc-Tg: $n = 10$, baseline = 227 ± 21 µV, post-MD = 159 ± 22 µV, $P = 0.01$ by paired t test; Fig. 1*B*). As expected, adult P180 WT mice did not exhibit

Fig. 1. Arc-Tg mice exhibit juvenile-like OD plasticity well past the conventional critical period. (*A*) Schematic of recording site for VEPs in layer IV of binocular visual cortex. (*B*) At P30, both WT and Arc-Tg mice show a significant decrease in contra (closed-eye) VEP amplitude following MD (WT: $n = 7$, *$P = 0.03$; Arc-Tg: $n = 10$, *$P = 0.01$). Additionally, Arc-Tg mice exhibited a small but significant increase in ipsi (open-eye) VEPs (Arc-Tg: *$P = 0.008$). There is no significant difference between WT and Arc-Tg animals before or after MD. (*C*) At P180, only Arc-Tg mice exhibit a significant decrease in contra VEPs (Arc-Tg: $n = 6$, *$P = 0.02$). (*D*) Plot of the fractional change in ipsi (*x* axis) and contra (*y* axis) eye VEPs following MD (same data as in *B* and *C*). At P30, there is no significant difference between WT and Arc-Tg mice. However, at P180, there is a significant difference between the fractional change of WT and Arc-Tg mice following MD ($P = 0.03$). Data are represented as mean ± SEM.

depression of contra VEP amplitude after MD, reflecting the loss of juvenile plasticity. In sharp contrast, P180 Arc-Tg mice still exhibited a significant decrease in contra VEPs (WT: $n = 7$, baseline = 184 ± 19 µV, post-MD = 183 ± 20 µV, $P = 0.9$; Arc-Tg: $n = 6$, baseline = 208 ± 26 µV, post-MD = 136 ± 20 µV, $P = 0.02$ by paired t test; Fig. 1*C*), comparable to the decrease observed in WT juveniles. There was a significant treatment by genotype interaction, indicating that OD plasticity differs in Arc-Tg mice compared with WT mice ($P = 0.0092$, repeated measures ANOVA).

Because the chronic VEP method enables measurements of response strength in the same mouse before and after MD, we can also analyze the qualities of the OD shift by plotting the fractional changes in response magnitude to stimulation of the deprived contra eye and the nondeprived ipsilateral (ipsi) eye (19, 20). This analysis confirms that at P30, both WT and Arc-Tg mice exhibit robust and comparable levels of contra eye depression and a variable potentiation of the nondeprived ipsi eye [Fig. 1*D*, squares; WT: contra depression = 0.7 ± 0.1, ipsi potentiation = 1.4 ± 0.2; Arc-Tg: contra depression = 0.7 ± 0.1, ipsi potentiation = 1.3 ± 0.1; $P = 0.9$, multivariate ANOVA (MANOVA)]. There was, however, a significant difference in the qualities of OD plasticity in WT and Arc-Tg adult mice (Fig. 1*D*, circles). In WT mice, the OD shift was accounted for entirely by ipsi eye potentiation (Fig. 1*D*, open circles), whereas the shift in Arc-Tg mice (Fig. 1*D*, filled circles) was solely due to contra eye depression (WT: contra depression = 1.0 ± 0.01, ipsi potentiation = 1.3 ± 0.1; Arc-Tg: contra depression = 0.7 ± 0.1, ipsi potentiation = 0.9 ± 0.2; $P = 0.03$, MANOVA; Fig. 1*D*).

These data show that augmenting Arc levels in adult mice prolongs juvenile-like OD plasticity, as evidenced by deprivation-induced synaptic depression well past the conventional critical period in mice.

Activity-Dependent Arc Protein Expression Is High During the Critical Period and Low in Adulthood. We reasoned that if availability of Arc influences the qualities of OD plasticity, Arc expression might decline as the animal ages. In mouse visual cortex, Arc is first detected after eye-opening (~P14) and expression steadily increases until ~P30, corresponding to the age of peak sensitivity to MD (21). To determine whether Arc levels decline with age, WT or Arc-Tg mice were killed at P30 or P180. Basal Arc expression in visual cortex is highly variable under standard housing conditions (21); therefore, we housed mice in the dark for 24 h and then either killed them immediately ("dark" condition) or exposed them to light for 2 h ("light" condition) before euthanasia ($n = 6$ per group) (22). The brain was fixed and sectioned at 30 µm on a cryostat, and immunohistochemistry (IHC) was performed for Arc protein using a custom-made Arc antibody (Fig. S2) on sections of brain containing primary visual cortex. The integrated density of Arc-expressing cells in layer IV of visual cortex, where VEPs and LTD were recorded, was measured with the experimenter blinded to genotype and age (Fig. 2*A*). A three-way ANOVA comparing genotype (WT or Arc-Tg), age (P30 or P180), and condition (dark or light) revealed a main effect of genotype ($P < 0.0001$), age ($P = 0.02$), and condition ($P < 0.0001$), as well as a genotype × condition interaction ($P = 0.02$). Post hoc Student's t tests showed that in P30 mice, light significantly induced Arc expression in both WT and Arc-Tg mice (WT: light > dark; light: 4.5 ± 1.3, dark: 1 ± 0.6, $P = 0.02$; Arc-Tg: light > dark; light: 8.2 ± 1, dark: 2.7 ± 2.7, $P = 0.002$). However, Arc-Tg mice expressed significantly more Arc after light exposure than WT mice ($P = 0.008$). At P180, WT mice no longer exhibited detectable Arc expression, even after light exposure. Arc-Tg mice, on the other hand, exhibited significant Arc expression after light exposure (light: 7.1 ± 0.8, dark: 1.8 ± 1.2; $P = 0.001$). Furthermore, levels of light-induced Arc in P180 Arc-Tg mice were not significantly different from P30 Arc-Tg mice ($P > 0.05$), suggesting that activity-dependent expression of Arc in Arc-Tg mice does not decline with
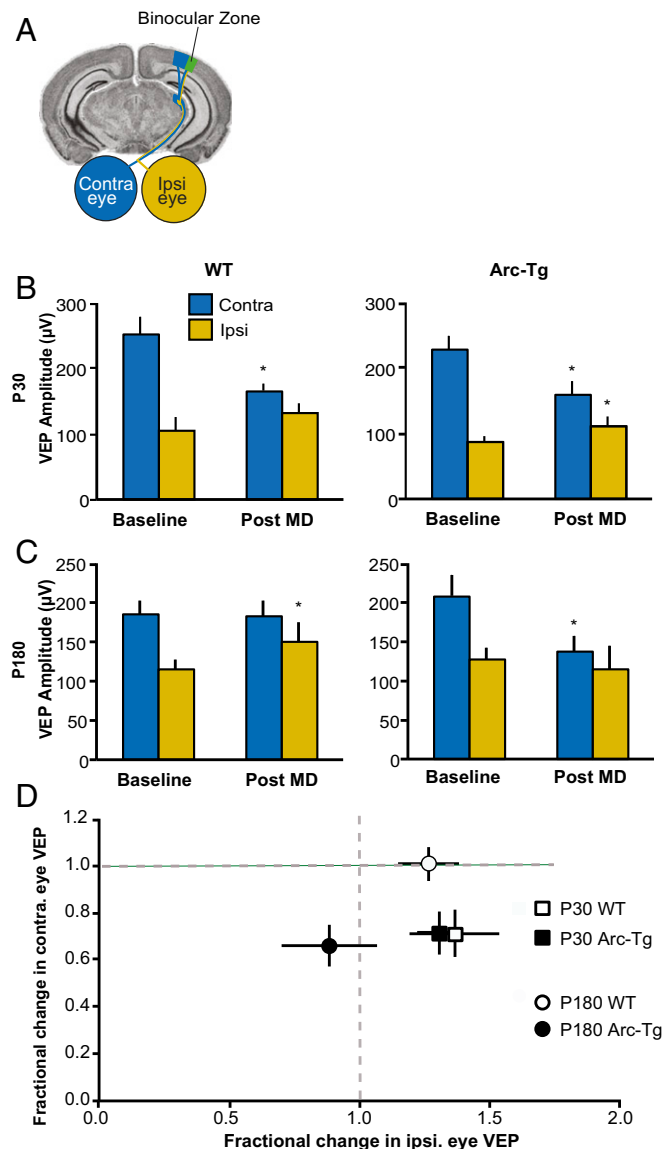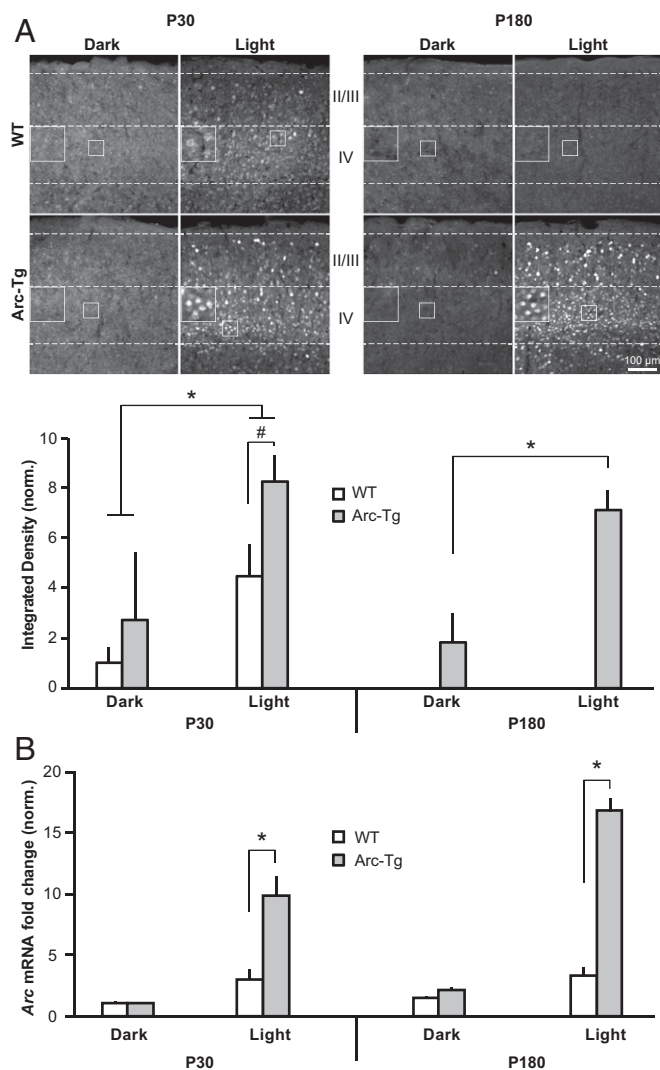
Fig. 2. Activity-dependent Arc protein, but not mRNA expression, declines with age in WT mouse visual cortex, but not in Arc-Tg mice. (*A*) IHC for Arc expression in layers I–IV of visual cortex after 24 h of being housed in the dark or 24 h of dark housing followed by 2 h of light exposure. Layer IV Arc expression is quantified in the graphs (*n* = 6 per group). Light increased Arc expression in both WT and Arc-Tg mice at P30 (WT: **P* = 0.02, Arc-Tg: **P* = 0.002), but Arc levels were higher in Arc-Tg mice (*#P* = 0.008). At P180, WT mice did not express Arc after light exposure, while Arc-Tg mice exhibited the same light-induced increase in Arc observed at P30 (**P* = 0.001). (Scale bar: 100 μm.) (*B*) WT and Arc-Tg mice were dark-housed for 24 h and then either killed in the dark (dark condition) or exposed to light for 2 h before euthanasia (light condition). qRT-PCR was run on dissected visual cortex to quantify *Arc* mRNA expression. All values were first normalized to GAPDH to control for total RNA levels. Light-induced *Arc* mRNA expression was higher in Arc-Tg mice than WT mice at both P30 and P180 (P30: **P* < 0.0001, P180: **P* < 0.0001). However, light-induced mRNA expression did not decrease with age in WT mice. Plotted data are normalized to P30 WT dark (*n* = 5 for WT light, *n* = 4 for Arc-Tg light, and *n* = 3 for all dark groups). Data are represented as mean ± SEM.

age. These data show that activity-dependent Arc protein expression significantly declines with age in WT but not Arc-Tg mice. This loss of endogenous Arc protein over age correlates with the decline of deprived-eye depression following MD.

Arc transcription and translation are exquisitely regulated in the brain and are finely tuned to experience and neuronal activity (12). Of particular interest, transcription and translation of Arc can be independently regulated by activity (23). We therefore sought to determine whether endogenous activity-dependent *Arc* mRNA expression also declines with age. Mice underwent dark and light exposure as described above (*n* = 3–5 per group). The visual cortex was dissected and qRT-PCR, the most sensitive and quantitative method of RNA detection, was performed on lysates (Fig. 2*B*). A three-way ANOVA revealed a main effect of genotype (*P* = 0.002) and condition (*P* = 0.0002), but not age. Post hoc *t* tests showed that light-induced *Arc* mRNA expression was higher in Arc-Tg than WT mice (P30 WT: 2.9 ± 0.9, P30 Arc-Tg: 9.8 ± 1.6, *P* < 0.0001; P180 WT: 3.3 ± 0.7, P180 Arc-Tg: 16.7 ± 1.1, *P* < 0.0001). Interestingly, however, levels of activity-induced *Arc* mRNA expression did not differ with age in either genotype (*P* > 0.05). Although we cannot rule out the possibility that analysis of layer IV alone would reveal an age effect, we note that Arc protein cannot be detected in any layer of V1 in adult WT mice. These data suggest that availability of endogenous *Arc* mRNA alone cannot fully explain the differences in Arc protein expression across the lifespan of WT mice and point to the possibility of a decrease in either activity-dependent translation or stability of endogenous Arc protein in adult visual cortex. Nevertheless, the increased expression of *Arc* mRNA in the active visual cortex of Arc-Tg mice is paralleled by a proportional increase in protein.

Augmenting Arc Expression Restores LTD in Adult Visual Cortex. Deprived-eye depression occurs via mechanisms shared with LTD (3), which also diminishes with age (24). In addition to the profound deficit in OD plasticity (11), juvenile (P20–25) Arc knockout (KO) mice exhibit impaired layer IV LTD in visual cortex, induced in slices with low-frequency stimulation (LFS) of the white matter, compared with WT mice, which showed robust LFS LTD (WT: *n* = 7 slices from four mice, 67.5 ± 5.7%; Arc KO: *n* = 7 slices from five mice, 90.6 ± 4.6%; *P* < 0.001, *t* test; Fig. 3*A*). We therefore hypothesized that the persistence of juvenile OD plasticity in adult Arc-Tg mice was accompanied (and perhaps accounted for) by continued expression of juvenile-like LTD. To ensure expression of Arc protein in the slices, mice were exposed briefly (30 min) to an enriched environment before euthanasia as described previously (23). We first measured LTD in juvenile mice when both WT and Arc-Tg animals show comparable OD plasticity, characterized by robust deprived-eye depression after MD. Over the age range examined, between P26 and P41, LTD in WT and Arc-Tg mice was also comparable (WT: *n* = 9 slices from seven mice, 75.4 ± 11.6%; Arc-Tg: *n* = 7 slices from six mice, 81.3 ± 7.1%; *P* > 0.5, *t* test; Fig. 3*B*). Subgroup analysis of this juvenile cohort revealed no difference in LTD in animals of either genotype at P26–33 or P34–41 (Fig. 3*B*, circles and inverted triangles, respectively). However, in adult mice (P180–200), we observed significant LTD in Arc-Tg slices but not in WT littermate slices (WT: *n* = 11 slices from six mice, 102.8% ± 8.7; Arc-Tg: *n* = 12 slices from six mice, 74.5 ± 7.9%; Fig. 3*C*). The difference between genotypes was significant (*P* = 0.04, *t* test). Thus, augmented expression of Arc in adult visual cortex restores or maintains two features of juvenile plasticity: LTD in vitro (Fig. 3*C*) and deprived-eye depression following MD in vivo (Fig. 1*C*).

Inhibition of Protein Synthesis in Vivo Impairs LTD in Juvenile Visual Cortex. The apparent requirement of Arc translation for deprived-eye depression may offer a partial explanation for why juvenile OD plasticity following brief MD is impaired when the visual cortex is infused locally with the protein synthesis inhibitor cycloheximide (CHX) (25). If this explanation is correct, and the mechanisms of LTD are used for deprived-eye depression following MD, we would also expect to observe reduced LTD ex vivo following microinfusion of CHX into visual cortex. To test this prediction, WT visual cortex was infused in vivo via an osmotic minipump with CHX for 4 d as described (25), and slices were then prepared to conduct LTD experiments. Similar to our observations in the Arc KO visual cortex, there was no LTD in juvenile visual cortex after chronic inhibition
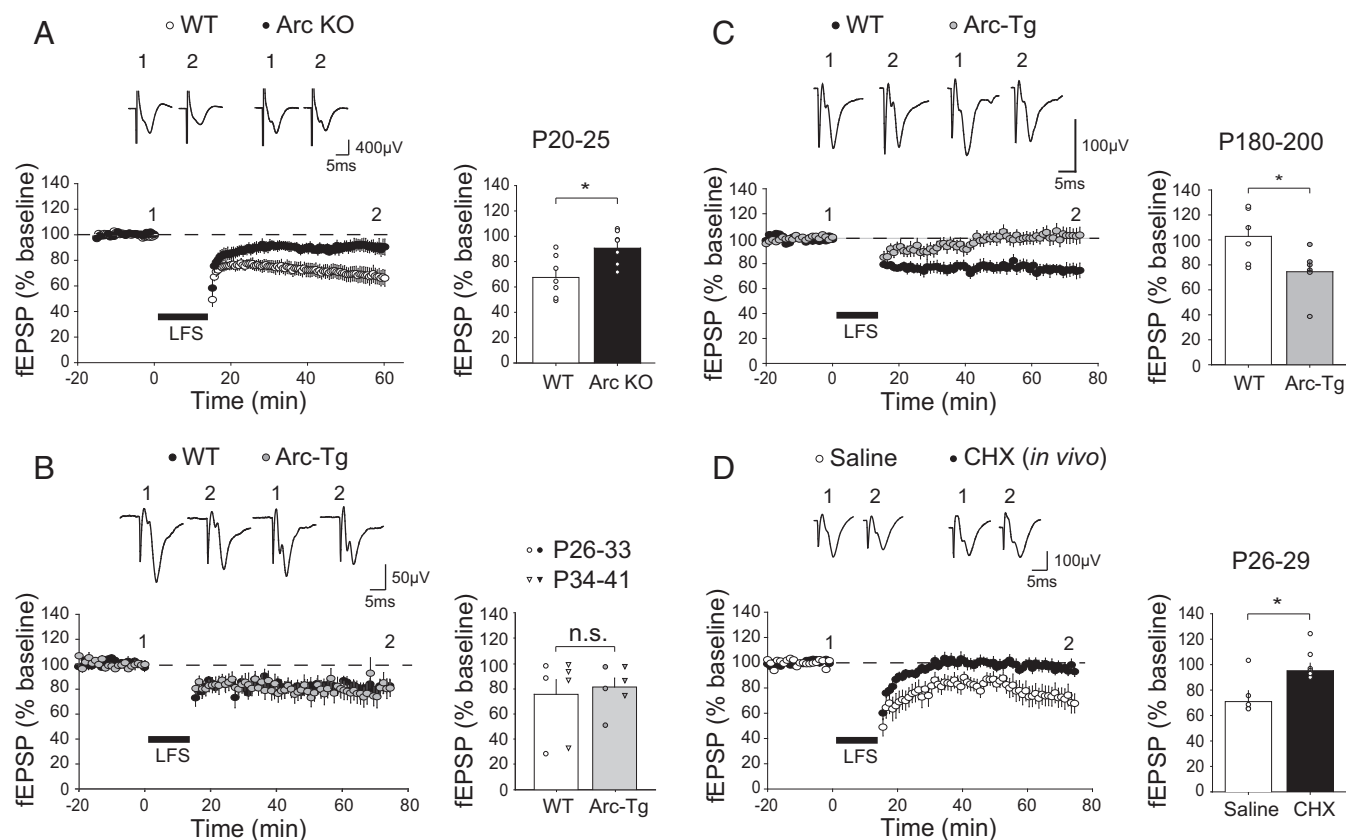
Fig. 3. Arc and protein translation are required for LTD in layer IV of visual cortex. (*A*) LFS (900 stimuli at 1 Hz) induces robust LTD in juvenile (P20–25) WT, but not Arc-KO, slices (average of last 5 min of recordings normalized to the baseline; WT: $n = 4$ mice, KO: $n = 5$; *$P < 0.001$). (*B*) LFS induces LTD to the same degree in young (P26–41) WT and Arc-Tg slices (WT: $n = 7$, Arc-Tg: $n = 6$; $P > 0.5$). The LTD amplitudes of field excitatory postsynaptic potential (fEPSP) of the youngest animals in this group (P26–33, circles) and the older animals (P34–41, inverted triangles) do not show any significant difference ($P > 0.5$, t test), and were therefore combined. (*C*) LFS induces robust LTD in adult (P180–200) Arc-Tg slices, but not WT slices (WT: $n = 11$, Arc-Tg: $n = 6$; *$P = 0.04$). (*D*) LFS induced LTD in juvenile (P25–30) visual cortex previously infused with saline, but not in visual cortex infused with CHX (saline: $n = 5$, CHX: $n = 5$; *$P = 0.02$). Data are represented as mean ± SEM.

of protein synthesis (saline: $n = 5$ slices from five mice, 72.4 ± 8.6%; CHX: $n = 7$ slices from five mice, 96.2 ± 5.9%; $P = 0.02$, t test; Fig. 3*D*). Together, these findings are consistent with the hypothesis that translation of Arc gates the mechanism of deprivation-induced synaptic depression in visual cortex.

Acute Expression of Arc in Adult Mouse Visual Cortex Is Sufficient to Reopen the Critical Period of Juvenile OD Plasticity. Augmenting the availability of Arc protein throughout development and into adulthood prolongs the critical period for juvenile OD plasticity (Fig. 1). However, this does not address whether restoring Arc protein expression is sufficient to reopen the critical period of OD plasticity once it has closed. To determine whether acutely increasing Arc protein in adult visual cortex is sufficient to restore juvenile-like plasticity, we expressed Arc using a lentivirus injected into visual cortex of P180 WT mice, which robustly increased Arc levels (Fig. 4*A* and Fig. S3). Lentivirus containing GFP-Arc or GFP was injected into layer IV of visual cortex, and baseline VEP recordings were conducted 1 wk after virus injection. Unlike the case in Arc-Tg mice, viral Arc overexpression is constitutively driven and not activity-dependent. Based on previous studies (26, 27), we predicted that VEP amplitude might be depressed by constitutive Arc expression since the VEP is mainly a synaptic population response that correlates with surface AMPA receptor expression (11). Indeed, a significant decrease in overall binocular VEP amplitude was observed compared with GFP-injected mice (GFP-injected mice: 197 ± 30 μV, GFP-Arc–injected mice: 75 ± 21 μV;

$P = 0.005$; Fig. 4*B*). No deprived-eye depression was observed in GFP-injected mice following short (3–4 d) MD (GFP: normalized to baseline contra values: $n = 11$; contra baseline = 1 ± 0.2, post-MD = 0.9 ± 0.2; $P = 0.4$, paired t test; Fig. 4*C*). However, despite a reduction in baseline VEP magnitude, contra VEP responses were further reduced after MD in GFP-Arc–injected mice (GFP-Arc: normalized to baseline contra values: $n = 5$, contra baseline = 1 ± 0.2, post-MD = 0.6 ± 0.2; $P = 0.02$; Fig. 4*D*). Further, when comparing the fractional change in contra eye and ipsi eye visual responses following MD, there was a significant difference between GFP- vs. GFP-Arc–injected mice (GFP: contra depression = 0.9 ± 0.1, ipsi potentiation = 1.4 ± 0.1; GFP-Arc: contra depression = 0.5 ± 0.1, ipsi potentiation = 1.0 ± 0.1; $P = 0.01$, MANOVA; Fig. 4*E*). Critically, the fractional OD shift in the P180 GFP-injected mice was the same as in noninjected WT P180 mice ($P = 0.3$, MANOVA), indicating virus injection had no effect on cortical responses or OD plasticity. Additionally, the fractional OD shift in P180 WT mice injected with GFP-Arc did not significantly differ from age-matched Arc-Tg mice, indicating that acute viral expression of Arc can restore OD plasticity to a degree similar to that achieved by Tg augmentation of Arc throughout life ($P = 0.6$, MANOVA; Fig. 4*E*). Intriguingly, not only was contra eye depression observed in Arc-Tg and GFP-Arc–injected mice but a lack of ipsi eye potentiation was also observed, further suggesting that Arc protein levels control the qualitative aspects of OD plasticity.

These data show that acutely increasing Arc protein expression in visual cortex is sufficient to restore juvenile OD plasticity
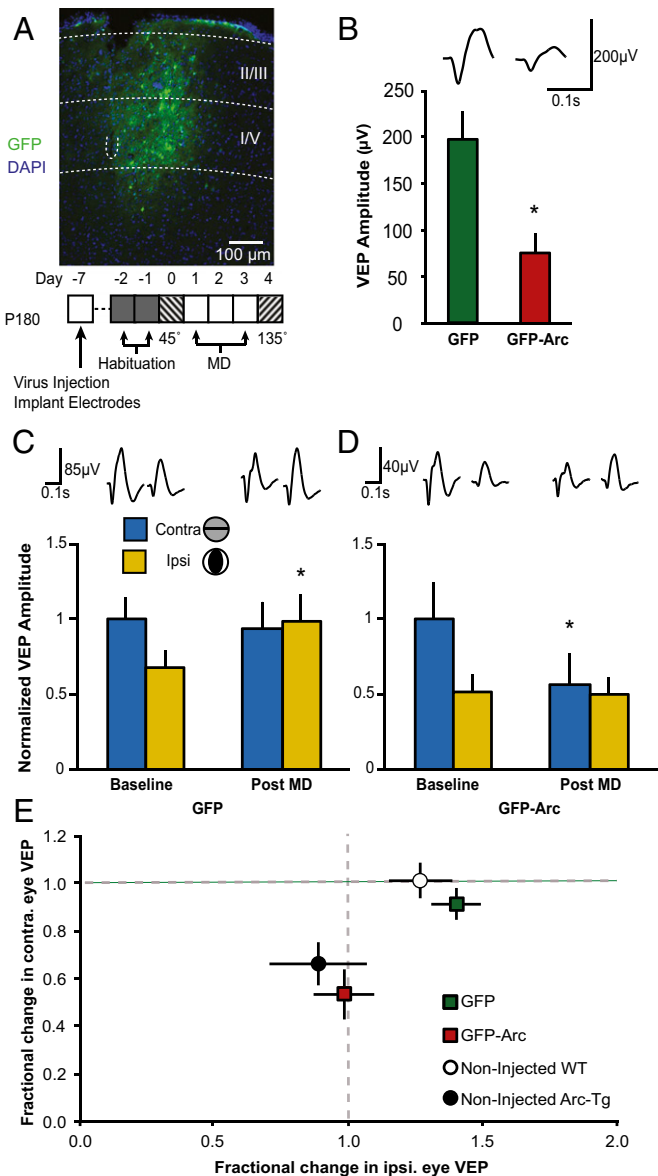
NEUROSCIENCE

in adult visual cortex, suggesting the increased availability of Arc protein is sufficient to allow deprivation-induced synaptic depression in adult visual cortex.

Discussion

Here, we show that acute or chronic up-regulation of Arc protein in adult mice renders visual cortical synapses sensitive to deprived-eye depression following MD, recapitulating juvenile critical period OD plasticity. In agreement with the prevailing hypothesis that LTD mechanisms mediate deprived-eye depression (3), overexpression of Arc also prolongs juvenile-like LTD in adult visual cortex. Conversely, elimination of Arc expression or inhibition of mRNA translation in juvenile visual cortex prevents deprived-eye depression after MD in vivo (11, 25) and LTD ex vivo. Together, these data indicate that availability of Arc is critical for the expression of juvenile plasticity in visual cortex.

Considering the key role for Arc in determining the qualities of OD plasticity in visual cortex of juvenile animals, we predicted that the loss of deprived-eye depression after MD in adult visual cortex correlates with a lack of activity-dependent Arc expression. Indeed, we found that endogenous Arc protein expression in the active visual cortex declines with age, coincident with the loss of juvenile plasticity. Surprisingly, however, we found that activity-dependent *Arc* mRNA expression is comparable in juvenile (~P30) and adult (~P180) WT mouse visual cortex. This finding implies that the normal decline in Arc protein expression in active visual cortex results from a decrease in experience-dependent *Arc* translation, which can occur via mechanisms that are distinct from those regulating activity-dependent transcription (12, 23). The lack of decline in activity-dependent Arc expression in Arc-Tg mice could be due to the increase in *Arc* mRNA levels. Alternatively or in addition, the extra *Arc* allele in the Arc-Tg line does not contain an intron in the 3′ UTR region, which may result in an increase in mRNA stability in dendrites due to a lack of nonsense-mediated decay (28), and would thus potentially have a longer half-life than endogenous *Arc* mRNA. Restoration of juvenile plasticity in adult mice injected with GFP-Arc suggests that the presence of Arc protein in visual cortex is sufficient for juvenile OD plasticity.

Deprived-eye depression after MD is believed to occur via mechanisms revealed by the study of LTD in layer IV. LTD in this layer is triggered by NMDA receptor activation and expressed by internalization of AMPA receptors (29). Although NMDA receptor-dependent LTD is not affected by acute (in vitro) inhibition of protein synthesis (30), we discovered that chronic inhibition of protein synthesis by in vivo microinfusion of CHX, which has been shown to prevent deprived-eye depression (25), impairs layer IV LTD ex vivo. These findings are reminiscent of the recent observation that chronic, but not acute, inhibition of metabotropic glutamate receptor 5 (mGluR5) can disrupt both deprived-eye depression after MD and LTD in layer IV (19). Activity-dependent synthesis of Arc protein occurs downstream of mGluR5 activation (12, 23). Thus, a simple explanation for this constellation of findings is that NMDA receptor-dependent LTD and deprived-eye depression require Arc protein as a necessary cofactor, and are inhibited by chronic block of either mGluR5 or protein synthesis. Decreased availability of Arc, and a consequent down-regulation of the mechanisms of LTD, also offers a simple molecular explanation for the age-dependent loss of synaptic sensitivity to visual deprivation.

Inhibition develops later than excitatory transmission in the cortex, and it has been suggested that the consequent decrease in the ratio of excitation to inhibition brings the critical period for juvenile plasticity to a close (10). We propose that decreasing the excitability of the visual cortex ultimately affects OD plasticity by preventing the activity-dependent expression of key activity-regulated plasticity proteins at the synapse that are important mediators of excitatory synaptic modification, such as Arc (Fig. S4).

Fig. 4. Acute Arc expression in adult mouse visual cortex is sufficient to restore juvenile OD plasticity. P180 WT mice were injected unilaterally in the visual cortex with lentivirus expressing either GFP alone or GFP-Arc. (*A*) Representative image of virally driven GFP expression in binocular visual cortex and time line of the experiment. The white dashed lines demarcate the cortical layers, as well as the position of the tip of the recording electrode. (*B*) GFP- and GFP-Arc–injected P180 mice were visually stimulated before MD with both eyes open to record binocular baseline VEPs. GFP-Arc–injected mice had significantly smaller VEPs than GFP-injected mice (GFP: *n* = 11, GFP-Arc: *n* = 5; *P* = 0.005). Traces represent average VEPs for GFP- and GFP-Arc–injected mice. (*C*) Data were normalized to baseline contra values. There was no significant change in contra VEP amplitudes following MD in GFP-injected animals (*P* > 0.05); however, there was a significant ipsi increase (*P* = 0.003). (*D*) Data were normalized to baseline contra values. GFP-Arc–injected mice exhibited significant contra depression following MD (*P* = 0.016) and no change in ipsi responses. Averaged VEP traces are presented above the graphs. (*E*) Plot of the fractional change in ipsi (*x* axis) and contra (*y* axis) eye VEPs following MD (same data as in C and D, noninjected WT and Arc-Tg data are from Fig. 1*B*). There is a significant difference between the fractional change in visual responses between GFP- and GFP-Arc–injected mice (*P* < 0.01). GFP-injected mice exhibit the same lack of change as noninjected P180 WT mice (*P* = 0.3), while GFP-Arc–injected mice exhibit the same degree of change as noninjected P180 Arc-Tg mice (*P* = 0.6). Data are represented as mean ± SEM.

Indeed, in addition to manipulations of inhibition, OD plasticity can be restored in adult rodents exposed to an enriched visual environment (6, 7), treated chronically with fluoxetine (8), or genetically engineered to express constitutively active CREB (31), manipulations that also increase Arc protein levels (32). The precise regulation of Arc expression during development therefore provides a potential mechanistic link between the maturation of inhibition and changes in the qualities of excitatory synaptic modification over the lifespan.

Materials and Methods

Animals. Tg mouse lines harboring the Arc-promoter mCherry-Arc transgene (mCherry-Arc/Arc) were generated as previously described (18). Further details can be found in *SI Materials and Methods*. Requests for mice should be directly addressed to H.B. or H.O. Arc KO mice were obtained from Kuan Wang, NIH, Bethesda, and were previously described (22). Both male and female mice were used, and the experimenter was blinded to genotype in all experiments. Male C57BL/6 mice (Charles River Laboratories) at the age of P22–25 were used for the Alzet pump implantation experiments. Male C57BL/6 mice (The Jackson Laboratory) at the age of P180 were used for lentiviral VEP experiments. All procedures were approved by the Institutional Animal Care and Use Committees of the Massachusetts Institute of Technology, the University of Utah, and The University of Tokyo Graduate School of Medicine, in conjunction with NIH guidelines.

Virus Production/Injection.

Virus production. Kimberly Huber, University of Texas Southwestern Medical Center, Dallas, generously donated FUGW lentiviral plasmids for ubiquitin (Ubq)-GFP and Ubq-GFP-Arc. Injections were carried out as previously described (33).

VEP recordings, slice electrophysiology, and IHC. VEP recordings, slice electrophysiology, and IHC were carried out as previously described (11, 19). Detailed methods on IHC, qRT-PCR, VEP recordings, and slice electrophysiology can be found in *SI Materials and Methods*.

Statistics. ANOVA/MANOVA tests and post hoc Student's *t* tests were performed using JMP Pro software (v12; SAS Institute). For slice electrophysiology experiments, post hoc paired *t* tests were performed to determine the significance of changes before and after LFS and unpaired *t* tests were performed to test the differences between groups after LFS.

1. Hübener M, Bonhoeffer T (2014) Neuronal plasticity: Beyond the critical period. *Cell* 159:727–737.
2. Espinosa JS, Stryker MP (2012) Development and plasticity of the primary visual cortex. *Neuron* 75:230–249.
3. Cooke SF, Bear MF (2013) How the mechanisms of long-term synaptic potentiation and depression serve experience-dependent plasticity in primary visual cortex. *Philos Trans R Soc Lond B Biol Sci* 369:20130284.
4. Hensch TK, et al. (1998) Local GABA circuit control of experience-dependent plasticity in developing visual cortex. *Science* 282:1504–1508.
5. Choi SY, Morales B, Lee HK, Kirkwood A (2002) Absence of long-term depression in the visual cortex of glutamic acid decarboxylase-65 knock-out mice. *J Neurosci* 22:5271–5276.
6. Greifzu F, et al. (2014) Environmental enrichment extends ocular dominance plasticity into adulthood and protects from stroke-induced impairments of plasticity. *Proc Natl Acad Sci USA* 111:1150–1155.
7. Matthies U, Balog J, Lehmann K (2013) Temporally coherent visual stimuli boost ocular dominance plasticity. *J Neurosci* 33:11774–11778.
8. Maya Vetencourt JF, et al. (2008) The antidepressant fluoxetine restores plasticity in the adult visual cortex. *Science* 320:385–388.
9. Hensch TK, Fagiolini M (2005) Excitatory-inhibitory balance and critical period plasticity in developing visual cortex. *Prog Brain Res* 147:115–124.
10. Jiang B, Huang ZJ, Morales B, Kirkwood A (2005) Maturation of GABAergic transmission and the timing of plasticity in visual cortex. *Brain Res Brain Res Rev* 50:126–133.
11. McCurry CL, et al. (2010) Loss of Arc renders the visual cortex impervious to the effects of sensory experience or deprivation. *Nat Neurosci* 13:450–457.
12. Shepherd JD, Bear MF (2011) New views of Arc, a master regulator of synaptic plasticity. *Nat Neurosci* 14:279–284.
13. Shepherd JD, et al. (2006) Arc/Arg3.1 mediates homeostatic synaptic scaling of AMPA receptors. *Neuron* 52:475–484.
14. Frenkel MY, Bear MF (2004) How monocular deprivation shifts ocular dominance in visual cortex of young mice. *Neuron* 44:917–923.
15. Sawtell NB, et al. (2003) NMDA receptor-dependent ocular dominance plasticity in adult visual cortex. *Neuron* 38:977–985.
16. Sato M, Stryker MP (2008) Distinctive features of adult ocular dominance plasticity. *J Neurosci* 28:10278–10286.
17. Kawashima T, et al. (2009) Synaptic activity-responsive element in the Arc/Arg3.1 promoter essential for synapse-to-nucleus signaling in activated neurons. *Proc Natl Acad Sci USA* 106:316–321.
18. Okuno H, et al. (2012) Inverse synaptic tagging of inactive synapses via dynamic interaction of Arc/Arg3.1 with CaMKIIβ. *Cell* 149:886–898.
19. Sidorov MS, Kaplan ES, Osterweil EK, Lindemann L, Bear MF (2015) Metabotropic glutamate receptor signaling is required for NMDA receptor-dependent ocular dominance plasticity and LTD in visual cortex. *Proc Natl Acad Sci USA* 112:12852–12857.
20. Dölen G, et al. (2007) Correction of fragile X syndrome in mice. *Neuron* 56:955–962.
21. Tagawa Y, Kanold PO, Majdan M, Shatz CJ (2005) Multiple periods of functional ocular dominance plasticity in mouse visual cortex. *Nat Neurosci* 8:380–388.
22. Wang KH, et al. (2006) In vivo two-photon imaging reveals a role of arc in enhancing orientation specificity in visual cortex. *Cell* 126:389–402.
23. Jakkamsetti V, et al. (2013) Experience-induced Arc/Arg3.1 primes CA1 pyramidal neurons for metabotropic glutamate receptor-dependent long-term synaptic depression. *Neuron* 80:72–79.
24. Dudek SM, Friedlander MJ (1996) Developmental down-regulation of LTD in cortical layer IV and its independence of modulation by inhibition. *Neuron* 16:1097–1106.
25. Taha S, Stryker MP (2002) Rapid ocular dominance plasticity requires cortical but not geniculate protein synthesis. *Neuron* 34:425–436.
26. Rial Verde EM, Lee-Osbourne J, Worley PF, Malinow R, Cline HT (2006) Increased expression of the immediate-early gene arc/arg3.1 reduces AMPA receptor-mediated synaptic transmission. *Neuron* 52:461–474.
27. Chowdhury S, et al. (2006) Arc/Arg3.1 interacts with the endocytic machinery to regulate AMPA receptor trafficking. *Neuron* 52:445–459.
28. Giorgi C, et al. (2007) The EJC factor eIF4AIII modulates synaptic strength and neuronal protein expression. *Cell* 130:179–191.
29. Crozier RA, Wang Y, Liu CH, Bear MF (2007) Deprivation-induced synaptic depression by distinct mechanisms in different layers of mouse visual cortex. *Proc Natl Acad Sci USA* 104:1383–1388.
30. Huber KM, Kayser MS, Bear MF (2000) Role for rapid dendritic protein synthesis in hippocampal mGluR-dependent long-term depression. *Science* 288:1254–1257.
31. Pham TA, et al. (2004) A semi-persistent adult ocular dominance plasticity in visual cortex is stabilized by activated CREB. *Learn Mem* 11:738–747.
32. Li Y, et al. (2015) Reversal of age-associated cognitive deficits is accompanied by increased plasticity-related gene expression after chronic antidepressant administration in middle-aged mice. *Pharmacol Biochem Behav* 135:70–82.
33. Kaplan ES, et al. (2016) Contrasting roles for parvalbumin-expressing inhibitory neurons in two forms of adult visual cortical plasticity. *Elife* 5:e11450.

NEUROSCIENCE

Supporting Information

Jenks et al. 10.1073/pnas.1700866114

SI Materials and Methods

Animals. Plasmid construction of pGL4.11-Arc7000-mCherry-Arc-UTRs was described previously (18). The plasmid was linearized and purified after removal of vector sequences. Tg mouse lines harboring the Arc promoter mCherry-Arc transgene (Arc-mCherry/Arc) were generated by microinjection of the purified DNA fragment into the pronucleus of fertilized C57BL/6 mouse eggs. Genomic integration of the transgene and reporter expression were analyzed by PCR, Southern blotting, Western blotting, and histological assays. Among several lines that showed activity-dependent expression of mCherry-Arc, one line that exhibited high reporter expression in the neocortex was selected and used for this study. Genotypes were identified by PCR with the following specific primers: arcpromoter3 (5′-GAGCCTGCCACACTCGCTAA-3′) and mcherry-tg3-2 (5′-TCAAGTAGTCGGGGATGTCG-3′). Requests for mice should be addressed directly to H.B. or H.O. Arc KO mice were obtained from Kuan Wang, NIH, Bethesda, and were previously described (22). Male C57BL/6 mice and female mCherry-Arc-Tg mice were bred together, yielding WT and Arc-Tg hemizygous (one allele of the transgene) littermates. Heterozygous Arc KO mice were bred together to yield WT and KO offspring. Both male and female mice were used, and the experimenter was blinded to genotype in all experiments. Male C57BL/6 mice (Charles River Laboratories) at the age of P22–25 were used for the Alzet pump implantation experiments. Male C57BL/6 mice (The Jackson Laboratory) at the age of P180 were used for lentiviral VEP experiments. All procedures were approved by the Institutional Animal Care and Use Committees of the Massachusetts Institute of Technology, the University of Utah, and The University of Tokyo Graduate School of Medicine, in conjunction with NIH guidelines.

IHC. WT and Arc-Tg mice at P30 and P180 were dark-housed for 24 h and either killed in the dark ("dark" condition) or exposed to light for 2 h and then killed ("light" condition). Brains were dissected out and fixed in 4% paraformaldehyde for 24 h, and then cryoprotected in 30% sucrose. Brains were sectioned on a cryostat at 30 μm and stored in cryoprotectant at −20 °C until needed. Sections containing visual cortex were blocked in 2% fish gelatin (Sigma–Aldrich)/5% normal donkey serum (Jackson ImmunoResearch)/0.1% Triton X-100 (Amresco) for 2 h, stained for Arc (custom-made antibody; ProteinTech) overnight at room temperature, and washed three times for 10 min each time in 1× PBS plus 2% fish gelatin. Slides were then incubated in secondary antibody (donkey anti-rabbit Alexa Fluor 488; Jackson ImmunoResearch) for 4 h and washed three times for 10 min each time in 1× PBS before being mounted on slides and coverslipped in Fluoromount mounting media (Sigma–Aldrich). A 10-section (1,272 × 1,272-μm) z-stack (each plane 2 μm apart) of binocular V1 for each mouse was acquired using a 10× objective on a confocal microscope (FV1000; Olympus). Sections used from each mouse had the same coordinates relative to bregma (−3.39 mm) to control for location of binocular V1 and cortical thickness. A maximum intensity projection of the z-stack was created in ImageJ (NIH). Every maximum intensity projection image was thresholded to the same level, and the integrated density of Arc-positive cells in layer IV was measured. Layer IV was determined by measuring 250 μm down from the dorsal cortical surface and then applying a 200-μm-tall × 900-μm-wide region of interest to measure the integrated density of only layer IV neurons.

qRT-PCR. P30 and P180 WT and Arc-Tg mice were dark-housed for 24 h and then either killed in the dark (dark condition) or exposed to 2 h of light (light condition) before euthanasia. Brains were removed, visual cortices were isolated and homogenized in TRIzol Reagent (Thermo Fisher Scientific), and RNA was isolated following the manufacturer's guidelines. Reverse transcription was performed using a High Capacity cDNA Reverse Transcription Kit (Thermo Fisher Scientific). qPCR was then performed using PowerUP SYBR Green Master Mix (Thermo Fisher Scientific). Analysis was performed by fitting the average of duplicate cycle threshold (Ct) values to a linear curve obtained from a serial dilution series for each primer set. Ct values for Arc from each cDNA sample, corresponding to RNA extracted from the visual cortex of one mouse, were normalized to GAPDH values run in parallel. Primers for amplification of murine Arc and GAPDH are listed below (5′ → 3′): Arc forward: GGA GGG AGG TCT TCT ACC GTC, Arc reverse: CCC CCA CAC CTA CAG AGA CA, GAPDH forward: CAT GGC CTT CCG TGT TCC TA, and GAPDH reverse: GCC TGC TTC ACC ACC TTC TT.

VEP Recordings.

Electrode implantation. Mice were anesthetized with an i.p. injection of ketamine (50 mg/kg) and xylazine (10 mg/kg), and a local anesthetic of 1% lidocaine hydrochloride (0.1 mL) was injected over the scalp. Petrolatum ophthalmic ointment (Dechra Pharmaceuticals) was applied to protect the eyes. The scalp was sterilized by alternately applying Betadine and 70% alcohol. For purposes of head fixation, a post was fixed to the skull just anterior to bregma using cyanoacrylate and a further application of dental cement. Two small (<0.5 mm) burr holes were made in the skull overlying the binocular visual cortex (3 mm lateral to lambda), and tungsten microelectrodes (FHC) were inserted ~450 μm below the cortical surface along the dorsal-ventral stereotaxic axis, positioning the electrode tip in cortical layer IV. Reference electrodes were placed bilaterally in prefrontal cortex. Electrodes were secured in place using cyanoacrylate, and the entire exposed area of skull was covered with dental cement. Animals were maintained at ~37 °C throughout the procedure and recovery, and general condition and reflex signs were monitored closely. Mice were monitored postoperatively for signs of infection or discomfort, and were allowed at least 24 h for recovery before habituation to the restraint apparatus. All animals were killed after the last recording session and processed for histology to determine the precise location of the recording electrode and virus expression (if injected).

Recording procedure. VEP recordings were conducted in awake mice. Mice were habituated to the restraint apparatus before the first recording session. The mice were alert and still during recording. Visual stimuli were presented to left and right eyes randomly. A total of 200 stimuli were presented per condition.

Visual stimuli. Visual stimuli consisted of full-field sine wave gratings (0.05 cycles per degree) of varying contrast (0–100%) generated by a VSG2/2 card (Cambridge Research Systems) and presented on a computer monitor suitably linearized by γ-correction. VEPs were elicited by horizontal, vertical, or oblique (45° or 135°) bars. The display was positioned 20 cm in front of the mouse and centered on the midline, thereby occupying 92° × 66° of the visual field. Mean luminance, determined by a photodiode placed in front of the computer screen, was 27 cd/m^2.

Analysis. VEP amplitude was quantified by measuring the trough-to-peak response amplitude of the average VEP waveform, as described previously (14). The fractional change in contra and ipsi

eye VEP amplitude was calculated as the VEP amplitude following MD divided by the VEP amplitude before MD, as described previously (20).

Virus Production/Injection.

Virus production. Kimberly Huber, University of Texas Southwestern Medical Center, Dallas, generously donated FUGW lentiviral plasmids for Ubq-GFP and Ubq-GFP-Arc. Lentiviral and packaging plasmids were transfected into HEK293 cells using FuGENE transfection reagent (Promega Corporation). Supernatant was collected 48–72 h posttransfection, spun at $3,000 \times g$ at 4 °C, and then passed through a 0.45 µm filter. Filtered supernatant was then centrifuged at $75,000 \times g$ to pellet the virus. After drying the pellet, virus was resuspended in ice-cold PBS and stored at −80 °C. The viral titer for each virus ranged from 8 to $9 * 10^7$ genome copies per milliliter.

Virus injection. The experimenter was blinded to the viruses being injected before surgery. P180 WT mice (C57BL/6J) were used for these experiments. Virus injection was carried out during electrode implantation surgery (discussed above), after drilling of the burr hole over binocular visual cortex and before lowering the electrode. Injection was done using a Nanoject II Auto-Nanoliter Injector (Drummond Scientific). A pulled glass pipette was backfilled with mineral oil before being attached to the Nanoject II. Virus was then loaded through the tip of the pipette. The pipette tip was lowered ~450 µm below the cortical surface and allowed to rest for 5 min. One microliter of virus was injected over 25 min. The pipette was left in place for 5 min before being withdrawn, and electrode implantation was completed as described above. To quantify relative Arc expression in GFP- and GFP-Arc–injected mice, a subset of mice did not receive electrodes and were killed 11 d following viral injection (corresponding to the end of the MD experiments). Brains were prepared for Arc IHC as described above, using a donkey anti-rabbit Alexa Fluor 555 (Jackson ImmunoResearch) secondary antibody. The integrated density of Arc-positive cells in layer IV was measured in binocular visual cortex as described above.

Slice Electrophysiology.

Slice preparation. WT or Arc KO mouse slices were prepared from juvenile P25–40 animals. For WT or Arc-Tg slice experiments, both P26-41 and P180-200 WT and Arc-Tg mice were exposed for 30 min to a 45×24-cm arena with toys and walls covered with stripes to ensure Arc expression (23) before receiving isoflurane anesthesia, followed by acute decapitation. Three hundred fifty-micrometer slices of visual cortex were made in high-sucrose dissection buffer containing 87 mM NaCl, 2.5 mM KCl, 1.25 mM NaH$_2$PO$_4$, 25 mM NaHCO$_3$, 0.5 mM CaCl$_2$, 7 mM MgCl$_2$, 75 mM sucrose, 10 mM dextrose, and 1.3 mM ascorbic acid. Slices recovered for 15 min at 32 °C, and then for at least 1 h at room temperature, in carbogenated artificial cerebrospinal fluid containing 124 mM NaCl, 5 mM KCl, 1.23 mM NaH$_2$PO$_4$, 26 mM NaHCO$_3$, 10 mM dextrose, 1 mM MgCl$_2$, and 2 mM CaCl$_2$ before recordings began.

Recordings. Extracellular field potential recordings were conducted using an interface chamber for Arc KO experiments and a submersion chamber for Arc-Tg slice experiments. A two-contact cluster microelectrode (FHC) was placed in white matter, a glass recording pipette was placed in cortical layer IV, and extracellular field potentials (40–50% of maximal response amplitude) were recorded. Baseline was collected at 0.03 Hz, and recordings were included only when the baseline drift was less than 5% over 30 min. LTD was induced by applying 900 pulses at 1 Hz for 15 min. The last 5 min of baseline and post-LFS recordings were averaged, and statistical comparisons were performed to determine the magnitude of LTD using two-tailed t tests.

Alzet pump implantation. P22–25 mice were anesthetized with ketamine (50 mg/kg) and xylazine (10 mg/kg,) i.p. and placed in a stereotaxic holder. Petrolatum ophthalmic ointment was applied to protect the eyes. Alzet micro-osmotic pumps (0.25 µL·h^{-1}, no. 1002; Durect Corp) were filled with either saline or CHX (10 mg/mL; Sigma–Aldrich) and connected to brain infusion cannulae (Alzet brain infusion kit 3). The scalp was sterilized by alternately applying Betadine and 70% alcohol, and 0.1 mL of lidocaine (2%) was applied under the scalp before scalp incision. A midline incision (1–1.5 cm) was made in the scalp, and the skin and connective tissue were retracted. Following incision, a lidocaine (2%) and epinephrine (1:50,000) solution was applied to the periosteum to avoid excessive bleeding or discomfort. A small burr hole was made in the skull (0.1 mm anterior, 2.7 mm lateral to lambda) with a dental drill through which an infusion cannula was lowered (450 µm below the dura mater). Cannulae were fixed to the skull by applying instant adhesive (Loctite 454). The attached mini-pump was placed in an s.c. pocket at the nape of the neck. The rest of the exposed scalp was covered with dental cement to hold the cannula in place and prevent inflammation. Animals were maintained at ~37 °C throughout the procedure and recovery, and general condition and reflex signs were monitored closely. Chemical infusion through the implanted pump continued for 5 d following surgery.
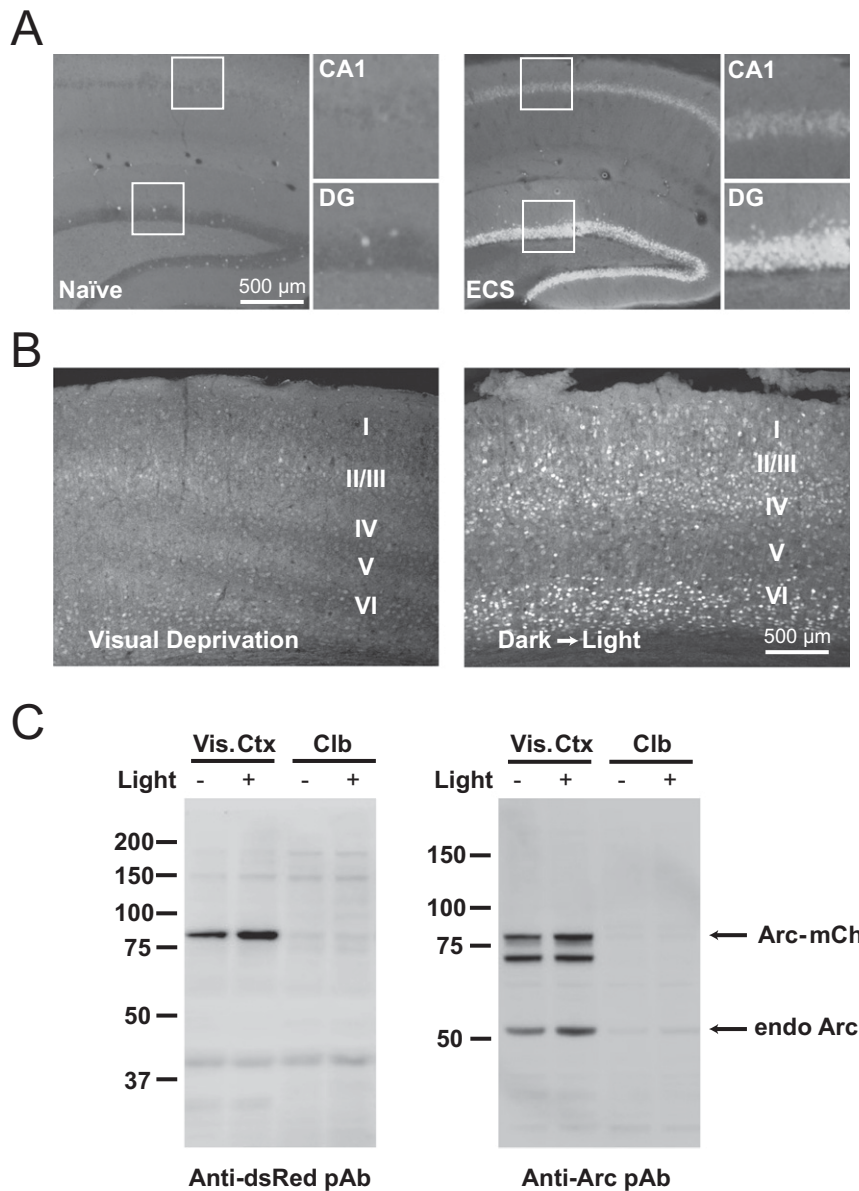
Fig. S1. Characterization of Arc-Tg mouse line. (*A, Left*) Arc-mCherry transgene mirrors endogenous Arc expression. In the hippocampus, basal expression of Arc-mCherry is low in both area CA1 and the dentate gyrus (DG). (*Insets*) Magnified CA1 and DG. (*A, Right*) Following electroconvulsive shock (ECS), levels of Arc-mCherry expression are dramatically increased in CA1 and DG, consistent with previous findings of ECS-induced induction of endogenous Arc. (Scale bar: 500 μm.) (*B*) Arc-mCherry transgene in the primary visual cortex reliably reports visual experience. (*Left*) P30 mouse dark-housed for 24 h (visual deprivation) has low levels of Arc-mCherry expression in all layers of visual cortex. (*Right*) P30 mouse dark-housed and then exposed to light for 2 h before euthanasia has increased levels of Arc-mCherry expression in the input layers of the visual cortex (layers II/III, IV, and VI). (*C*) Visually driven Arc-mCherry (mCh) expression is specific to visual areas and recapitulates endogenous (endo) Arc expression. Dark-housed mice (Light −) had little Arc-mCherry and endogenous Arc expression in visual cortex (Vis. Ctx) compared with light-exposed mice (Light +), as assessed by antibodies against mCherry (Anti-DsRed pAb) and Arc. This effect of light exposure was specific to the visual system, as both basal and light-induced Arc-mCherry and native Arc expression was equally low in the cerebellum (Clb).
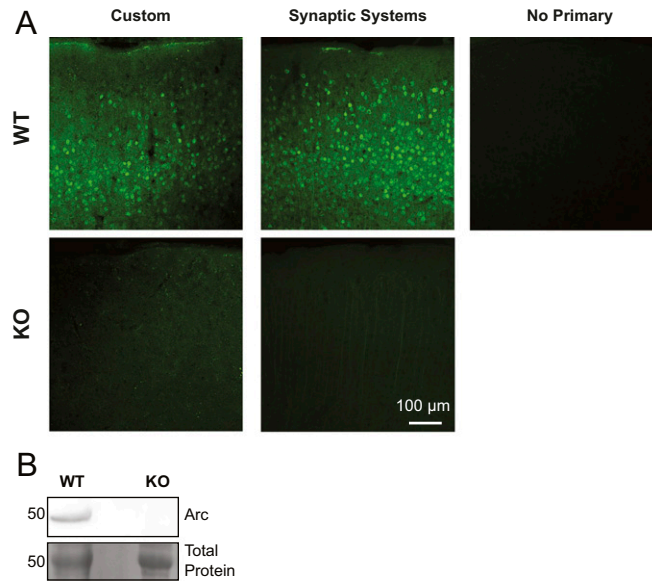
Fig. S2. Validation of custom Arc antibody. (*A*) Side-by-side comparison of custom Arc antibody and commercially available Arc antibody (catalog no.156-003; Synaptic Systems). Custom and commercial Arc antibodies show comparable levels of staining in WT P30 mouse visual cortex (*Upper Left* and *Center*) and comparable levels of background in Arc KO P30 mouse visual cortex (*Lower Left* and *Center*). (*Upper Right*) WT tissue not stained with a primary antibody for comparison. (*B*) Western blot of visual cortex lysates from a P30 WT and Arc KO mouse stained with the custom Arc antibody. Arc is detected in WT, but not Arc KO, lysate.
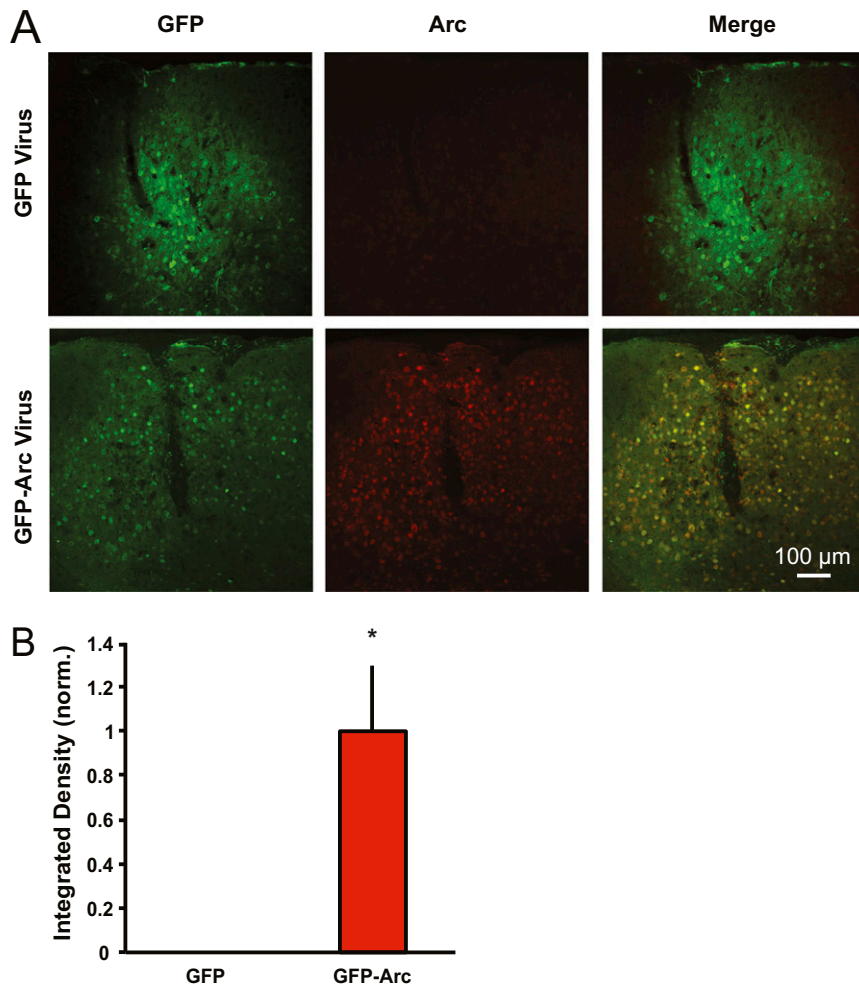
Fig. S3. GFP-Arc lentivirus increases Arc expression in P180 WT visual cortex. P180 WT mice were injected unilaterally in the visual cortex with lentivirus expressing either GFP alone or GFP-Arc. (*A*) Representative images from visual cortex of a mouse injected with GFP lentivirus (*Upper*) and a mouse injected with GFP-Arc lentivirus (*Lower*). (*Left* and *Middle*) GFP expression from GFP and GFP-Arc lentiviruses (no antibody staining) is shown. (*Right*) IHC for Arc expression is shown. (*B*) Quantification of Arc expression from GFP- and GFP-Arc–injected mice (four GFP-injected, four GFP-Arc–injected). When images were set to a threshold determined by the maximum Arc expression in GFP-Arc–injected mice, there was no detectable Arc expression in layer IV of GFP-injected mice above background staining, as seen in noninjected P180 WT (Fig. 2). However, there was a significant increase in Arc expression in GFP-Arc–injected mice ($P = 0.02$, Student t test). Data are normalized (norm.) to GFP and displayed as mean ± SEM.
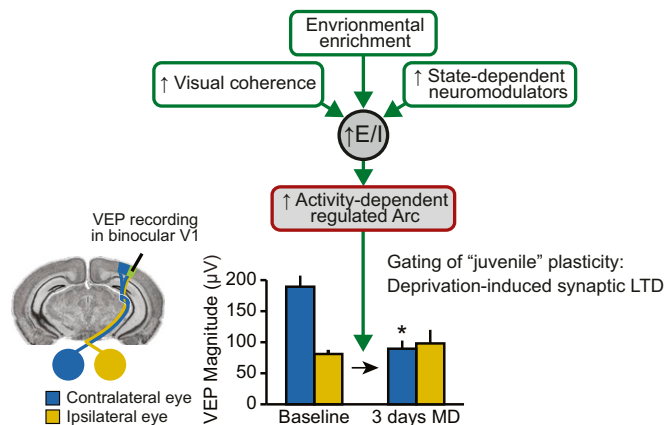

Fig. S4. Model of Arc's role in controlling the "juvenile" quality of OD plasticity. Various genetic, environmental, and pharmacological manipulations have been shown to promote juvenile-like plasticity in adult visual cortex. It has been proposed that these manipulations cause a general increase in the ratio of excitation (E) to inhibition (I). Here, we propose that the increase in E/I restores juvenile plasticity specifically by allowing the induction of activity-regulated genes such as Arc. Increased Arc expression promotes activity-dependent synaptic depression that underlies juvenile OD plasticity. *Significantly lower than contralateral eye at baseline.